optica

Generation of intensity-controlled two-dimensional shape-preserving beams in plasmonic lossy media

Itai Epstein,[1,*] Roei Remez,[1] Yuval Tsur,[1] and Ady Arie[1,2]

[1]Department of Physical Electronics, School of Electrical Engineering, Fleischman Faculty of Engineering, Tel Aviv University, Tel Aviv 69978, Israel
[2]e-mail: ady@post.tau.ac.il
*Corresponding author: itayet@post.tau.ac.il

Received 21 August 2015; revised 11 November 2015; accepted 16 November 2015 (Doc. ID 248415); published 24 December 2015

Two-dimensional surface-plasmon polariton waves, which propagate at a metal/dielectric interface, exhibit unique and attractive properties. These extraordinary properties, however, are accompanied by fundamentally inherent losses. The latter is probably the most pronounced challenge in the field of plasmonics and a true bottleneck for many applications. Shape-preserving beams, on the other hand, are unique solutions of the wave equation; they maintain their shape with propagation and also possess the ability to self-reconstruct. Here, we study the first realization of surface-plasmon shape-preserving beams, which maintain their shape and intensity over long distances, even when subjected to plasmonic losses. Moreover, their intensity distribution along propagation can be arbitrarily tailored. This is achieved without the use of any gain media, but rather by strictly controlling the initial plasmonic wavefront. This approach can be valuable for a variety of plasmonic applications, such as surface particle trapping and manipulation, on-chip communication, nonlinear optics, and more.

OCIS codes: (240.6680) Surface plasmons; (090.0090) Holography; (140.3300) Laser beam shaping; (250.5403) Plasmonics.

http://dx.doi.org/10.1364/OPTICA.3.000015

1. INTRODUCTION

In the last two decades, surface-plasmon polaritons have attracted an enormous amount of scientific and technological interest owing to their unique properties [1–3]. They have been widely used in a variety of fundamental discoveries and applications, such as extraordinary transmission [4], focusing to sub-wavelengths [5], and manipulating Snell's and Bragg's fundamental laws [6,7]. Furthermore, surface plasmons can exist on arbitrary small metallic waveguides, and together with the advancements of nanofabrication technology, they have carried high hopes for bringing the next on-chip optical technologies [2,8–10]. However, the propagating surface-plasmon wave is inherently lossy [1], thus making it questionable for some practical applications. In recent years, increased effort has been made to overcome plasmonic losses. These include the use of various gain media, lasing, and hybrid waveguides [11–15]. However, a scientific debate regarding the efficiency of these solutions was raised, owing to the tradeoff between the degree of confinement and its associated loss [16–18].

In contrast to the lossy nature of plasmons, shape-preserving beams (SPBs) are solutions of Helmholtz's equation, and are "diffraction-free," i.e., they maintain their shape and intensity with propagation [19]. Moreover, they can "self-heal," i.e., self-reconstruct back into their original shape after passing through an obstacle [20]. The exact SPB solution carries infinite energy and is therefore non-square integrable. The best-known example of an SPB is the three-dimensional Bessel beam [19], which propagates along a straight trajectory in free space. However, in recent years, an increased interest has been focused on self-accelerating beams, i.e., SPBs that possess all the properties mentioned above, but propagate along curved trajectories, such as the Airy [21–24], half-Bessel [25], parabolic [26], Mathieu, and Weber beams [27,28]. While these wave solutions carry infinite energy, a modified finite-energy SPB, in which the infinite beam is multiplied by an envelope, such as a Gaussian function, enables one to observe all these unique properties, but over a finite, rather than an infinite, spatial extent [22,29]. In three-dimensional space, several studies have researched controlling the intensities of such beams in absorbing media, either by using straight propagating Bessel beams [30,31] or curved self-accelerating beams [32,33]. However, while most three-dimensional systems can be treated as loss free for most of the optical spectrum (visible and near-infrared ranges), the loss in two-dimensional (2D) plasmonic systems is inevitable for all wavelengths. Moreover, the previous pioneering realizations of similar plasmonic beams relied either on ad-hoc methods for generating specific beams [34], or phase-only methods, which have limited control over the plasmonic intensity profile [35].

In this article, we study the general behavior of 2D SPBs in plasmonic lossy media. We show that a careful analysis of the 2D case enables us to arbitrarily manipulate their propagation characteristics, thereby allowing us to control their longitudinal intensity in lossy media. This is achieved by gaining precise control over the initial plasmonic wavefront and its intensity, without the need for using gain materials, metamaterials, or other complex

structures. We provide a theoretical derivation for this general approach based on geometrical considerations, and demonstrate it experimentally for plasmonic SPBs propagating along straight trajectories, curved trajectories, and for highly localized plasmonic SPBs, extending over distances much longer than the plasmonic propagation length.

2. SHAPE-PRESERVING BEAMS IN LOSSY MEDIA

The analytical solution of an SPB is characterized by a transverse amplitude profile that is completely independent of the propagation coordinate. This characteristic leads to the unique non-diffracting and self-healing properties of SPBs in a loss-free medium. However, when propagating through lossy media, they will suffer an exponential decay of their intensity. Nevertheless, it is possible to arbitrarily design the intensity of the beam's inner lobes along the propagation direction, and over long distances, by transferring energy from its outer lobes. This variation in the intensity can be regarded as a minor change to the shape of the beam, as the spatial positions of both peaks and zeros of the beam's lobes remain unchanged. In that aspect, this enhanced SPB can still be regarded as being shape preserving. The 2D SPB equivalent of the three-dimensional Bessel beam is the cosine beam [34,36]. Its exact infinite solution can be described as an interference pattern of two infinite plane-waves, $E_1(z,y)$ and $E_2(z,y)$, where z and y are the longitudinal and transverse coordinates, respectively, propagating with a relative angle of 2θ with respect to one another [Fig. 1(b)]. In order to have a finite energy beam, this cosine beam is multiplied by a Gaussian envelope, leading to the cosine-Gaussian beam. In the case of a plasmonic cosine-Gaussian beam, both plane waves experience exponential decay with propagation, leading to an exponentially decaying beam [34]. In that case, the losses should also be taken into account in the derivation of the interference pattern. The field at point z has amplitudes of $|E_1(0,y)|e^{-k''d}$ and $|E_2(0,-y)|e^{-k''d}$ for the upward and downward propagating waves, respectively, where $d = z/\cos(\theta)$, is the distance between points $(0,\pm y)$ and $(z,0)$, and k'' is the imaginary part of the surface plasmon wave vector [(Fig. 1(c)]. Here, we assumed a slowly varying amplitude for fields E_1 and E_2; hence, the geometrical approximation holds. For simplicity, we focus our analysis on the central lobe of the plasmonic cosine beam, although the entire beam in the infinite case will exhibit the same characteristics (see Supplement 1). To obtain an enhanced cosine beam with an arbitrary intensity function, $A^2(z)$, along the propagation trajectory of the central lobe, it can be shown that under the geometrical approximation, the transverse field profile at $z = 0$ is (see Supplement 1)

$$E(z=0,y) = \frac{1}{2}A\left(\frac{y}{\tan(\theta)}\right)e^{k''y/\sin(\theta)}e^{ik'y\sin\theta} + \frac{1}{2}A\left(\frac{-y}{\tan(\theta)}\right)e^{-k''y/\sin(\theta)}e^{-ik'y\sin\theta}, \quad (1)$$

where k' is the real part of the surface-plasmon wave vector.

As mentioned above, the practical realization of this beam is based on multiplying the two interfering plane waves with a Gaussian envelope. This truncation of the beam will also lead to additional diffraction effects owing to its finite aperture, which in turn will lead to some decrease in intensity. However, one can show that this decrease is quite small for the plasmonic propagation length scales at hand, and therefore, these effects are negligible (see Supplement 1).

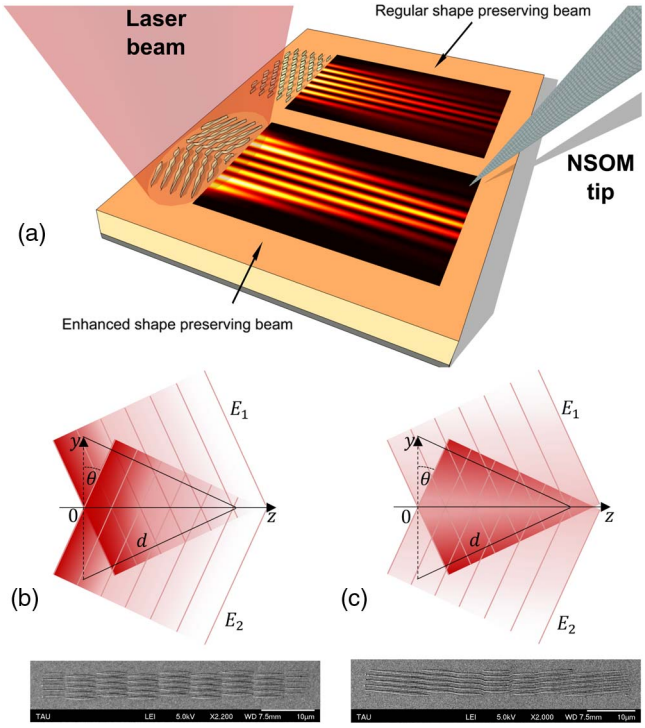

Fig. 1. (a) Apparatus: the designed plasmonic holograms are fabricated on a gold substrate and illuminated from free space by the laser beam. An NSOM then collects the near-field intensities of the generated plasmonic. (b) and (c) Geometrical construction of CG beams in lossy media by two plane-waves interference (top), $E_1(z,y)$ and $E_2(z,y)$, (color represents the intensity). For the regular CG in (b), both plane waves experience exponential decay, and the resulting CG beam will decay with propagation as well. For the constant intensity CG (c), the intensity of both plane waves is enhanced, thus enabling the beam to keep its intensity constant with propagation in spite of the exponential losses. A scanning electron microscope image of the plasmonic hologram that generates each one of the beams in (b) and (c) appears at the bottom.

The plasmonic cosine-Gaussian (CG) beam that was previously demonstrated was realized by illuminating two slanted gratings with a Gaussian beam, which provided the envelope function [34,37]. This approach is quite challenging in controlling the transverse field distribution, and therefore also in controlling the propagation characteristics of the generated plasmonic SPBs. To realize these unique plasmonic SPBs, it is mandatory to have a high level of control over the plasmonic wavefront, as delivering the precise amount of energy to the precise location is crucial in order to obtain the desired plasmonic arbitrary intensity, $A^2(z)$. To achieve this, we use a class of near-field plasmonic holograms that was recently introduced [38], which enables the excitation of any desired plasmonic beam whose 2D amplitude and phase distributions, $A(z,y)$, $\phi(z,y)$, are known. In our method, the truncation of the beam is done by encoding into the hologram the field in Eq. (1) multiplied by a super-Gaussian envelope, i.e., a cosine-super-Gaussian (CSG) beam. This allows to maintain a higher amount of energy within the beam compared to a Gaussian envelope. We note that as expected from finite SPBs, this truncation will distort the CSG properties closer to the edge. Conceptually, increasing the beam's aperture will also

increase the portion of the beam that keeps the desired behavior, and also increases the propagation distance over which this behavior is maintained.

3. EXPERIMENTAL RESULTS

In order to demonstrate the robustness of our approach, we chose gold as the lossy metal for its increased plasmonic losses (e.g., relative to silver). A silicon substrate was coated with 25 nm of Ti as an adhesion layer and 150 nm of gold film on top. The sample is then spin coated with a PMMA [polymethyl methacrylate] resist, and the plasmonic hologram is then written by standard electron-beam lithography. After development of the PMMA, an additional 50 nm of gold layer was evaporated on top of the PMMA pattern, followed by a lift-off process. For an operating wavelength of 1064 nm, the surface-plasmon propagation length at the air/gold interface, defined as the point where the intensity drops to a value of 1/e, is ∼100 μm. We illuminate the hologram with a focused laser beam and measure the generated plasmonic beam intensity using a near-field scanning optical microscope (NSOM) system [Fig. 1(a)]. We design the enhanced plasmonic SPBs to exhibit their properties over an 80 μm × 80 μm area, which corresponds to the scanning range limit of the NSOM system. This range is more than sufficient for demonstrating the control over the SPBs propagation characteristics compared to the ∼100 μm plasmonic propagation length. To verify the theoretical derivation presented above for the CSG beam and to predict the output of the plasmonic holograms, the intensity distribution of the generated plasmonic SPBs was simulated by a numerical calculation based on the 2D Green's function of the Helmholtz equation (see Supplement 1).

Figure 2 shows the numerical simulations and experimental measurements of three kinds of plasmonic CSG beams. The first is a regular plasmonic CSG beam, in which the central lobe decays exponentially with propagation, according to the plasmonic decay constant [Figs. 2(a), 2(d), and 2(g)]. The second is an enhanced plasmonic CSG beam in which the central lobe maintains its intensity with propagation, thereby exactly compensating for the plasmonic decay losses [Figs. 2(b), 2(e), and 2(h)]. The third is an enhanced plasmonic CSG beam in which the central lobe intensity increases linearly with propagation, thereby overcoming the plasmonic decay losses [Figs. 2(c), 2(f), and 2(i)]. The exhibited behavior of the central lobe of each beam is obtained by calculating its averaged intensity along the propagation trajectory [Figs. 2(g), 2(h), and 2(i)]. It is noticeable that the additional side lobes located near the central lobe of the bea, also exhibit this characteristic behavior, which gradually breaks from the desired behavior towards the edges of the beam. This behavior can be understood as the above-mentioned edge effects owing to the finite nature of the beam.

The ability to arbitrarily control the propagation characteristics of the generated plasmonic SPBs is clearly seen from Fig. 2, and although we chose these three specific examples, any arbitrary intensity distribution that holds up under the geometrical approximation can be realized, according to Eq. (1). As further examples, Figs. 3(a) and 3(b) present simulations of enhanced plasmonic CSG beams with more complex intensity distributions, and show a central-lobe intensity distribution for $A(z) = \cos(z)$ and $A(z) = z$, respectively.

We note that for faster compensation rates, and beams that are much wider than the central lobe, less energy will reside in the central area relative to the side lobes [Fig. 3(b)]. In addition, the

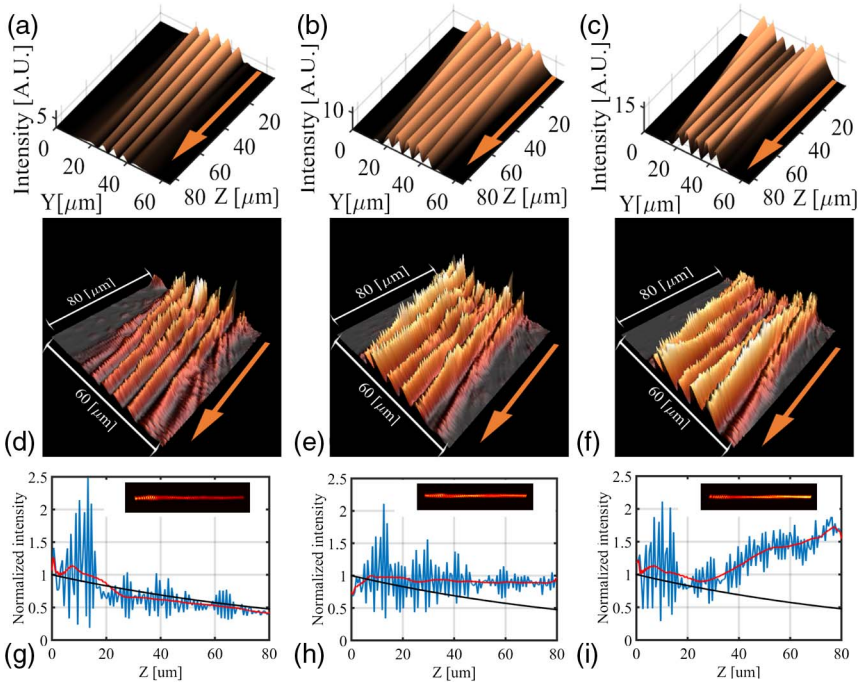

Fig. 2. Simulations of three kinds of plasmonic SPBs: (a) a regular plasmonic CSG, the intensity of which decays exponentially with propagation, (b) a plasmonic CSG exhibiting constant intensity with propagation, and (c) a plasmonic CSG exhibiting a linearly growing intensity with propagation (orange arrow represents the direction of propagation). (d)–(f) Three-dimensional representation of the experimentally measured intensities of the three beams in (a)–(c), respectively, exhibiting exponentially lossy, constant, and linearly growing intensity beams. (g)–(i) Averaged intensity behavior exhibited by the central lobe of each beam (blue/red curves), and its intensity distribution (insets) along 80 μm of propagation distance. The black line represents the plasmonic exponential decay at the air/gold interface for a wavelength of 1064 nm.

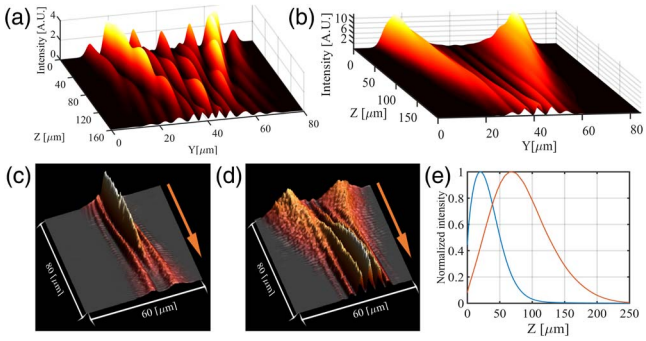

Fig. 3. Simulation of plasmonic CSG beams having (a) an $A(z) = \cos(z)$ and (b) an $A(z) = z$ distribution profile. (c) Experimental generation of a regular plasmonic LCSG beam, where its central lobe completely decays after 80 μm of propagation. (d) Experimental generation of an enhanced plasmonic LCSG beam, where its central lobe's intensity reaches the maximum level after 80 μm. (e) Simulated intensity of the central lobe of both regular and enhanced plasmonic LCSG beams along 300 μm of propagation distance, showing that the enhanced beam can propagate almost three times the distance of the regular beam.

finite width of the holograms themselves leads to the diffraction of the generated beam. A comprehensive study of these effects is presented in Supplement 1.

The cosine beam is an exact SPB solution of the 2D Helmholtz equation, and therefore can be analyzed and manipulated in a straightforward manner. However, it is beneficial to study the behavior of more localized beams, where a significant amount of energy is localized mainly in the central lobe of the beam. Among these are the local-cosine-Gaussian (LCG) beam [34], or the one-dimensional (1D) plasmonic Bessel beam, recently suggested in multilayered metal/dielectric structures, and analyzed for the cases of lossless [39] and lossy [40] metals. Similar to the CG beam, these can be regarded as SPBs, but only over a limited spatial range, regardless of the issue of truncation mentioned for exact infinite SPB solutions [34,41]. Still, within this limited range, our approach can be applied to produce well-defined and highly controllable results. The advantage of our approach can be clearly seen by the generation of an enhanced LCG [Figs. 3(c)–3(e)]. While the central lobe of the regular plasmonic LCG beam completely decays after 80 μm of propagation [Fig. 3(e)], that of the enhanced LCG beam peaks at 80 μm and extends over a distance that is around three times that of the regular beam. For comparison, applying our approach to the conditions of the original LCG generated by Lin *et al.* [34] also yields an extended propagation length of around three times the distance (see Supplement 1). In addition, our approach can also be applied for the generation of both regular and enhanced 1D plasmonic Bessel SPBs (see Supplement 1).

All that has been demonstrated so far for 2D straight-propagating plasmonic SPBs should also hold for 2D self-accelerating SPBs. Therefore, we have verified that our approach is indeed valid for these, and we have also experimentally generated three kinds of plasmonic self-accelerating paraxial Airy beams (Fig. 4): a regular Airy plasmon, which decays exponentially with propagation [Fig. 4(a)], an enhanced Airy plasmon, which maintains constant intensity with propagation [Fig. 4(b)], and an enhanced Airy plasmon, which exhibits an exponentially increasing intensity with propagation [Fig. 4(c)]. We note that the slight decrease in intensity in the middle of the main lobe in Figs. 4(b) and 4(c) is due the acceleration rate of the beam, which deviates from the

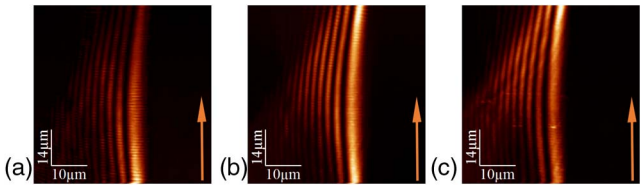

Fig. 4. (a) Experimental generation of a regular plasmonic self-accelerating Airy beam; its main lobe decays with propagation. (b) Experimental generation of an enhanced plasmonic self-accelerating Airy beam; its main lobe's intensity is kept constant with propagation. (c) Experimental generation of an enhanced plasmonic self-accelerating Airy beam; its main lobe's intensity increases exponentially with propagation.

paraxial approximation in order to show acceleration over an 80 μm propagation distance.

We also note that since the analytical solution presented here for the cosine beam does not hold for self-accelerating SPBs, controlling the intensity of their main lobe is achieved by manipulating the beam's decay constant beam, as in Schley *et al.* [32].

4. CONCLUSIONS

In conclusion, we have presented a study of 2D SPBs in plasmonic lossy media. We have shown that when appropriately controlled, these SPBs can maintain constant and even increasing longitudinal intensities, despite being subjected to plasmonic losses. Moreover, their propagation characteristics in lossy media can be arbitrarily designed. Although this demonstration focuses on 2D plasmonic SPBs, it can be readily applied to other waves propagating in lossy media, e.g., electron waves [42], acoustic waves [43], and even surface water waves [44]. The vast degree of freedom provided by our approach may enable the realization of important applications. In particular, our approach can be highly useful for on-chip communication and particle manipulation on a surface, where the intensity and the phase gradients must be strictly controlled, without the need for conveying liquids [45]. In addition, all that has been demonstrated here in the spatial domain can also be implemented in the time domain, thereby enabling the realization of enhanced light-bullet beams [46].

Funding. Israel Science Foundation (ISF) (1310/13).

See Supplement 1 for supporting content.

REFERENCES

1. S. Maier, *Plasmonics: Fundamentals and Applications* (Springer, 2007).
2. T. W. Ebbesen, C. Genet, and S. I. Bozhevolnyi, "Surface-plasmon circuitry," Phys. Today **61**(5), 44 (2008).
3. W. L. Barnes, A. Dereux, and T. W. Ebbesen, "Surface plasmon subwavelength optics," Nature **424**, 824–830 (2003).
4. T. W. Ebbesen, H. J. Lezec, H. F. Ghaemi, T. Thio, and P. A. Wolff, "Extraordinary optical transmission through sub-wavelength hole arrays," Nature **391**, 667 (1998).
5. D. K. Gramotnev and S. I. Bozhevolnyi, "Nanofocusing of electromagnetic radiation," Nat. Photonics **4**, 83–91 (2010).
6. N. Yu, P. Genevet, M. A. Kats, F. Aieta, J. P. Tetienne, F. Capasso, and Z. Gaburro, "Light propagation with phase discontinuities: generalized laws of reflection and refraction," Science **334**, 333 (2011).
7. I. Epstein, I. Dolev, D. Bar-Lev, and A. Arie, "Plasmon enhanced Bragg diffraction," Phys. Rev. B **86**, 205122 (2012).

8. J. Leuthold, C. Hoessbacher, S. Muehlbrandt, A. Melikyan, M. Kohl, C. Koos, W. Freude, V. Dolores-Calzadilla, M. Smit, I. Suarez, J. Martínez-Pastor, E. P. Fitrakis, and I. Tomkos, "Plasmonic communications: light on a wire," Opt. Photon. News **24**(5), 28 (2013).
9. H. A. Atwater, "The promise of plasmonics," Sci Am. **296**, 56–63 (2007).
10. M. L. Brongersma and V. M. Shalaev, "The case for plasmonics," Science **328**, 440 (2010).
11. P. Berini and I. De Leon, "Surface plasmon–polariton amplifiers and lasers," Nat. Photonics **6**, 16–24 (2012).
12. N. Sudarkin and P. A. Demkovich, "Excitation of surface electromagnetic waves on the boundary of a metal with an amplifying medium," Sov. Phys. Tech. Phys. **34**, 764–766 (1989).
13. D. Bergman and M. Stockman, "Surface plasmon amplification by stimulated emission of radiation: quantum generation of coherent surface plasmons in nanosystems," Phys. Rev. Lett. **90**, 027402 (2003).
14. J. Grandidier, G. C. des Francs, S. Massenot, A. Bouhelier, L. Markey, J.-C. Weeber, C. Finot, and A. Dereux, "Gain-assisted propagation in a plasmonic waveguide at telecom wavelength," Nano Lett. **9**, 2935–2939 (2009).
15. R. F. Oulton, V. J. Sorger, D. A. Genov, D. F. P. Pile, and X. Zhang, "A hybrid plasmonic waveguide for subwavelength confinement and long-range propagation," Nat. Photonics **2**, 496–500 (2008).
16. R. F. Oulton, "Plasmonics: loss and gain," Nat. Photonics **6**, 219–221 (2012).
17. J. B. Khurgin, "How to deal with the loss in plasmonics and metamaterials," Nat. Nanotechnol. **10**, 2–6 (2015).
18. J. B. Khurgin and A. Boltasseva, "Reflecting upon the losses in plasmonics and metamaterials," MRS Bull. **37**(8), 768–779 (2012).
19. J. Durnin, J. J. Miceli, Jr., and J. H. Eberly, "Diffraction-free beams," Phys. Rev. Lett. **58**, 1499 (1987).
20. Z. Bouchal, J. Wagner, and M. Chlup, "Self-reconstruction of a distorted nondiffracting beam," Opt. Commun. **151**, 207–211 (1998).
21. M. V. Berry and N. L. Balazs, "Nonspreading wave packets," Am. J. Phys. **47**, 264 (1979).
22. G. A. Siviloglou and D. N. Christodoulides, "Accelerating finite energy Airy beams," Opt. Lett. **32**, 979 (2007).
23. A. E. Minovich, A. E. Klein, D. N. Neshev, T. Pertsch, Y. S. Kivshar, and D. N. Christodoulides, "Airy plasmons: non-diffracting optical surface waves," Laser Photon. Rev. **8**, 221–232 (2014).
24. I. Epstein and A. Arie, "Arbitrary bending plasmonic light waves," Phys. Rev. Lett. **112**, 023903 (2014).
25. I. Kaminer, R. Bekenstein, J. Nemirovsky, and M. Segev, "Nondiffracting accelerating wave packets of Maxwell's equations," Phys. Rev. Lett. **108**, 163901 (2012).
26. M. A. Bandres, "Accelerating parabolic beams," Opt. Lett. **33**, 1678 (2008).
27. P. Zhang, Y. Hu, T. Li, D. Cannan, X. Yin, R. Morandotti, Z. Chen, and X. Zhang, "Nonparaxial Mathieu and Weber accelerating beams," Phys. Rev. Lett. **109**, 193901 (2012).
28. A. Libster-Hershko, I. Epstein, and A. Arie, "Rapidly accelerating Mathieu and Weber surface plasmon beams," Phys. Rev. Lett. **113**, 123902 (2014).
29. F. Gori, G. Guattari, and C. Padovani, "Bessel–Gauss beams," Opt. Commun. **64**, 491–495 (1987).
30. M. Zamboni-Rached, "Diffraction-Attenuation resistant beams in absorbing media," Opt. Express **14**, 1804–1809 (2006).
31. I. Golub, T. Mirtchev, J. Nuttall, and D. Shaw, "The taming of absorption: generating a constant intensity beam in a lossy medium," Opt. Lett. **37**, 2556–2558 (2012).
32. R. Schley, I. Kaminer, E. Greenfield, R. Bekenstein, Y. Lumer, and M. Segev, "Loss-proof self-accelerating beams and their use in non-paraxial manipulation of particles' trajectories," Nat. Commun. **5**, 5189 (2014).
33. M. A. Preciado, K. Dholakia, and M. Mazilu, "Generation of attenuation-compensating Airy beams," Opt. Lett. **39**, 4950–4953 (2014).
34. J. Lin, J. Dellinger, P. Genevet, B. Cluzel, F. de Fornel, and F. Capasso, "Cosine-Gauss plasmon beam: a localized long-range nondiffracting surface wave," Phys. Rev. Lett. **109**, 093904 (2012).
35. L. Li, T. Li, S. M. Wang, and S. N. Zhu, "Collimated plasmon beam: nondiffracting versus linearly focused," Phys. Rev. Lett. **110**, 046807 (2013).
36. J. C. Gutiérrez-Vega and M. A. Bandres, "Helmholtz-Gauss waves," J. Opt. Soc. Am. A **22**, 289–298 (2005).
37. C. Garcia-Ortiz, V. Coello, Z. Han, and S. Bozhevolnyi, "Generation of diffraction-free plasmonic beams with one-dimensional Bessel profiles," Opt. Lett. **38**, 905–907 (2013).
38. I. Epstein and A. Arie, "Shaping plasmonic light beams with near-field plasmonic holograms," J. Opt. Soc. Am. B **31**, 1642–1647 (2014).
39. C. J. Zapata-Rodríguez, S. Vuković, M. R. Belić, D. Pastor, and J. J. Miret, "Nondiffracting Bessel plasmons," Opt. Express **19**, 19572–19581 (2011).
40. C. J. Zapata-Rodríguez, D. Pastor, V. Camps, M. T. Caballero, and J. J. Miret, "Three-dimensional point spread function of multilayered flat lenses and its application to extreme subwavelength resolution," J. Nanophoton. **5**, 051807 (2011).
41. C. J. Regan, L. Grave de Peralta, and A. A. Bernussi, "Two-dimensional Bessel-like surface plasmon-polariton beams," J. Appl. Phys. **112**, 103107 (2012).
42. N. Voloch-Bloch, Y. Lereah, Y. Lilach, A. Gover, and A. Arie, "Generation of electron Airy beams," Nature **494**, 331–335 (2013).
43. P. Zhang, T. Li, J. Zhu, X. Zhu, S. Yang, Y. Wang, X. Yin, and X. Zhang, "Generation of acoustic self-bending and bottle beams by phase engineering," Nat. Commun. **5**, 4316 (2014).
44. S. Fu, Y. Tsur, J. Zhou, L. Shemer, and A. Arie, "Propagation dynamics of Airy water wave pulses," Phys. Rev. Lett. **115**, 034501 (2015).
45. M. Soltani, J. Lin, R. A. Forties, J. T. Inman, S. N. Saraf, R. M. Fullbright, M. Lipson, and M. D. Wang, "Nanophotonic trapping for precise manipulation of biomolecular arrays," Nat. Nanotechnol. **9**, 448–452 (2014).
46. A. Chong, W. H. Renninger, D. N. Christodoulides, and F. W. Wise, "Airy-Bessel wave packets as versatile linear light bullets," Nat. Photonics **4**, 103–106 (2010).